⌘ *Author's Choice*

THE JOURNAL OF BIOLOGICAL CHEMISTRY VOL. 285, NO. 4, pp. 2857–2866, January 22, 2010

The p53 Core Domain Is a Molten Globule at Low pH

FUNCTIONAL IMPLICATIONS OF A PARTIALLY UNFOLDED STRUCTURE[*] [S]

Received for publication, October 14, 2009, and in revised form, November 15, 2009 Published, JBC Papers in Press, November 17, 2009, DOI 10.1074/jbc.M109.075861

Ana Paula D. Ano Bom[‡§], Monica S. Freitas[‡§], Flavia S. Moreira[‡], Danielly Ferraz[‡§], Daniel Sanches[‡§], Andre M. O. Gomes[‡§], Ana Paula Valente[‡§], Yraima Cordeiro[§¶], and Jerson L. Silva[‡§1]

From the [‡]Centro Nacional de Ressonância Magnética Nuclear de Macromoléculas, Instituto de Bioquímica Médica, [¶]Faculdade de Farmácia, and [§]Instituto Nacional de Ciência e Tecnologia de Biologia Estrutural e Bioimagem, Universidade Federal do Rio de Janeiro, Rio de Janeiro, RJ 21941-590, Brazil

p53 is a transcription factor that maintains genome integrity, and its function is lost in 50% of human cancers. The majority of p53 mutations are clustered within the core domain. Here, we investigate the effects of low pH on the structure of the wild-type (wt) p53 core domain (p53C) and the R248Q mutant. At low pH, the tryptophan residue is partially exposed to the solvent, suggesting a fluctuating tertiary structure. On the other hand, the secondary structure increases, as determined by circular dichroism. Binding of the probe bis-ANS (bis-8-anilinonaphthalene-1-sulfonate) indicates that there is an increase in the exposure of hydrophobic pockets for both wt and mutant p53C at low pH. This behavior is accompanied by a lack of cooperativity under urea denaturation and decreased stability under pressure when p53C is in acidic pH. Together, these results indicate that p53C acquires a partially unfolded conformation (molten-globule state) at low pH (5.0). The hydrodynamic properties of this conformation are intermediate between the native and denatured conformation. ^{1}H-^{15}N HSQC NMR spectroscopy confirms that the protein has a typical molten-globule structure at acidic pH when compared with pH 7.2. Human breast cells in culture (MCF-7) transfected with p53-GFP revealed localization of p53 in acidic vesicles, suggesting that the low pH conformation is present in the cell. Low pH stress also tends to favor high levels of p53 in the cells. Taken together, all of these data suggest that p53 may play physiological or pathological roles in acidic microenvironments.

In the last decade, efforts toward finding a cure for cancer have identified many factors responsible for cancer development. Several proteins are related to the formation and development of tumors, including the tumor suppressor protein p53 (1). The tumor suppression activity of wild-type (wt)[2] p53 is mostly linked to its DNA binding properties (2). One of the major functions of p53 is to serve as a transcription factor that both positively and negatively regulates the expression of a large and disparate group of responsive genes (3). These genes have important roles in mediating cell-cycle arrest, senescence, and apoptosis (4). p53 function is lost in over 50% of human cancers, demonstrating the major role of this protein in tumorigenesis (5). Of the nearly 22,000 studied point mutations in p53, 97% are found in the core domain (p53C; residues 94–312). The six most frequent cancer-associated mutations are the "hot spot" mutations: R175H, G245S, R248Q, R249S, R273H, and R282W (6). Mutations at amino acids Arg-248 and Arg-273 lead to impaired DNA binding by p53 because these residues are in the DNA-contact interface (7). The crystal structure of the core domain bound to a consensus DNA sequence has provided a template for understanding the nature of mutant p53 (2).

The p53 protein possesses great flexibility and is able to bind several gene promoters during cell growth, which explains the population of alternative conformations (7, 8). It has been previously reported that when subjected to high hydrostatic pressure, wt p53C acquires a distinct folding resembling that of the R248Q p53C point mutation (9). This altered conformation aggregates at 37 °C to form amyloid-like deposits (10). p53C has maximum stability at pH 7.2 (11). Recently, we found that interaction with a cognate DNA sequence stabilizes p53 and prevents aggregation of the protein into an amyloid-like structure (12). These distinct conformations of p53C might be partially folded intermediate states of the folding pathway.

Several proteins have been demonstrated to exist in nonnative conformations (*e.g.* fully unfolded, partially unfolded, or molten-globular forms (13–18)). The molten globule (MG) state is a compact structure with a pronounced secondary structure, but it lacks tertiary structure (19–21). MGs have been suggested to be involved in many important physiological processes, including translocation and interaction with several molecules (19, 22–25). MG states may occur in the protein folding pathway at points of local energy minima (26). Many nonnative protein conformations are observed under mild denaturing conditions, such as incubation at moderately low or high pH, changes in pressure or temperature, variations in solution

* This work was supported by grants from Conselho Nacional de Desenvolvimento Científico e Tecnológico (CNPq), CNPq Millennium and National Insitute Programs, Fundação Carlos Chagas Filho de Amparo à Pesquisa do Estado do Rio de Janeiro (FAPERJ), Financiadora de Estudos e Projetos (FINEP), and Fundação Universitária José Bonifácio (FUJB) of Brazil.

⌘ *Author's Choice*—Final version full access.

[S] The on-line version of this article (available at http://www.jbc.org) contains supplemental Figs. S1 and S2.

[1] To whom correspondence should be addressed: Universidade Federal do Rio de Janeiro, Instituto de Bioquímica Médica, Bloco E Sala 10, Cidade Universitária, Rio de Janeiro, RJ 21941-590, Brazil. Tel.: 55-21-2562-6756; Fax: 55-21-3881-4155; E-mail: jerson@bioqmed.ufrj.br.

[2] The abbreviations used are: wt, wild type; DTT, dithiothreitol; HSQC, heteronuclear single quantum coherence; bis-ANS, bis-8-anilinonaphthalene-1-sulfonate; GFP, green fluorescent protein; CM, center of spectral mass; p53C, core domain of the tumor suppressor protein p53; MG, molten globule; MES, 4-morpholineethanesulfonic acid; GdmCl, guanidine hydrochloride.

ionic strength, or addition of chaotropic agents (21, 27–29). It has been shown that some DNA-binding proteins display a partially unfolded MG state (21, 30–32). A few tumor suppressor proteins and other tumor-related macromolecules present this dual behavior, including the von-Hippel Lindau tumor suppressor protein (pVHL) (18), the p300 CH1 domain bound to Zn^{2+} (22), and p16 protein mutants (33). Investigation of these conformational changes will provide information about the molecular mechanisms involved in protein structural conversion.

The present work demonstrates that wt p53C and the R248Q p53C mutant can adopt a molten globule structure at a slightly acidic pH. At pH 5.0, we characterized the structural and spectroscopic properties of this MG-like intermediate. Our results indicate that wt p53C and R248Q p53C display different folding characteristics at pH 5.0 and 7.2. Structural characterization of intermediate species in the protein folding pathway is an important challenge in understanding the protein folding mechanism (19, 20, 34–36) that may lead to a better understanding of pathological conditions like cancer. We further show that p53 can localize to acidic vesicles in human breast cells in culture, which makes the characterization of the protein folding state at low pH crucial. The tendency to form a molten globule is related to the protein structural flexibility and to the propensity to lose function or aggregate.

EXPERIMENTAL PROCEDURES

Chemicals—All reagents were of analytical grade. Distilled water was filtered and deionized through a Millipore water purification system. The bis-ANS probe was purchased from Molecular Probes (Eugene, OR). Experiments were performed using the following buffers: 20 mM acetate, pH 4.5; 70 mM acetate, pH 5.0; 50 mM MES, pH 5.5 to 6.5; and 50 mM Tris, pH 7.0 to 9.0. All buffers contained 150 mM NaCl, 5 mM DTT, and 5% (v/v) glycerol.

Subcloning, Expression, and Purification of wt p53C and R248Q—p53C (comprising amino acid residues 94–312) subcloning, expression, and purification was performed as previously described (9).

Circular Dichroism Measurements—CD experiments were carried out using a Jasco J-715 spectropolarimeter (Jasco Corporation, Tokyo, Japan) with a 2.0 mm path-length quartz cuvette. For determinations of spectra, wt or R248Q p53C was diluted in different buffers to a final concentration of 10 μM. Far-UV spectra were monitored from 200 to 260 nm, averaged over 3 scans at a speed of 50 nm/min, and collected in 0.2-nm steps. The buffer baselines were subtracted from their respective sample spectra.

Fluorescence Spectroscopy Measurements—Fluorescence measurements were carried out in an ISS-PC1 spectrofluorometer (Champaign, IL). The excitation wavelength was fixed at 278 nm, and the emission spectrum was recorded from 295 to 415 nm. Tryptophan and tyrosine fluorescence spectra were quantified as the center of the spectral mass ($<\upsilon>$) in Equation 1,

$$\langle \upsilon \rangle = \sum \upsilon_i \cdot F_i / \sum F_i \qquad \text{(Eq. 1)}$$

where F_i is the fluorescence emission at wave number ν_i, and the summation is carried out over the range of measured values of F. The temperatures used are described for each experiment. For experiments in the presence of bis-ANS, the excitation wavelength was fixed at 360 nm, and the fluorescence emission was collected from 400 to 600 nm.

HPLC Analysis—Gel filtration chromatography was performed using a Superdex 75 column (Amersham Biosciences) attached to a high-pressure liquid chromatography system (Shimadzu, Tokyo, Japan). wt p53C and R248Q at pH 5.0 were dialyzed for 18 h in the presence of 70 mM acetate, 150 mM NaCl, 5 mM DTT, and 5% (v/v) glycerol. For analysis at pH 7.2, samples were diluted in 50 mM Tris, 150 mM NaCl, 5 mM DTT, and 5% (v/v) glycerol. The samples (16 μM) were applied to a column previously equilibrated with the appropriate buffer at 25 °C. Runs were carried out at a flow rate of 1 ml/min with intrinsic fluorescence detection at 320 nm (excitation set at 280 nm) and absorbance recorded at 280 nm. The column was calibrated with standard proteins with known hydrodynamic radiuses.

NMR Data—^{1}H-^{15}N heteronuclear single quantum coherence (HSQC) measurements were performed at 20 °C at 600 MHz in a Bruker DRX600 spectrometer (Bruker Biospin GmbH, Rheinstetten, Germany) using a 5-mm inverse detection triple resonance probe with z gradient and with a cryoprobe (Bruker Biospin GmbH, Rheinstetten, Germany). Water suppression was achieved using the watergate technique (37). The proteins were concentrated and dialyzed in each buffer: 25 mM phosphate, 150 mM NaCl, and 2.5% (v/v) glycerol, pH 7.2 or 70 mM acetate, 150 mM NaCl, and 2.5% (v/v) glycerol, pH 5.0. To each purified p53C sample, 10% D_2O (Isotec., Miamisburg, OH) and 5 mM DTTd10 (Cambridge Isotope Laboratories Inc., Andover, MA) were added. The NMR data were processed with NMRpipe (38) and analyzed using NMRVIEW, version 5.0.3 (39). The ^{1}H-^{15}N HSQC spectra of the wild-type p53C were assigned according to Wong *et al.* (40).

Chemical Denaturation—The samples were incubated in the presence of different urea concentrations (1–9 M) in the appropriate buffer solution for 1 h or treated with high hydrostatic pressure (from 0.1 to 3 kbar). The fluorescence spectra were obtained using the same conditions described in "Fluorescence Spectroscopy Measurements." The exact concentrations of the stock solutions of urea were checked by refractive index measurement (41).

Western Blot Analysis—Protein extracts derived from MCF-7 cells (human breast adenocarcinoma cells) that expressed p53 were prepared in Laemmli SDS sample buffer, boiled for 5 min, and loaded onto an SDS-polyacrylamide gel (10%) (100 μg/well). After electrophoresis, the proteins were transferred to a polyvinylidene difluoride membrane using the X cell II blot system (Invitrogen). The blots were blocked with TBS-T buffer (10 mM Tris-HCl, 0.15 M NaCl, 8.0 pH, 0.1% Tween 20) and low fat milk (5%) for 2 h with continuous gentle agitation. The membranes were incubated with primary antibodies anti-p53 (D0–1), anti-GAPDH (sc-47724), or anti-MDM2 (sc-13161) (Santa Cruz Biotechnology), diluted 1:1000, for 18 h at 4 °C. The membranes were washed and then incubated with horseradish peroxidase (HRP)-conjugated mouse anti-human immunoglobulins at a 1:100,000 dilution for 1 h at room temperature (Roche Diagnostics). An x-ray film was

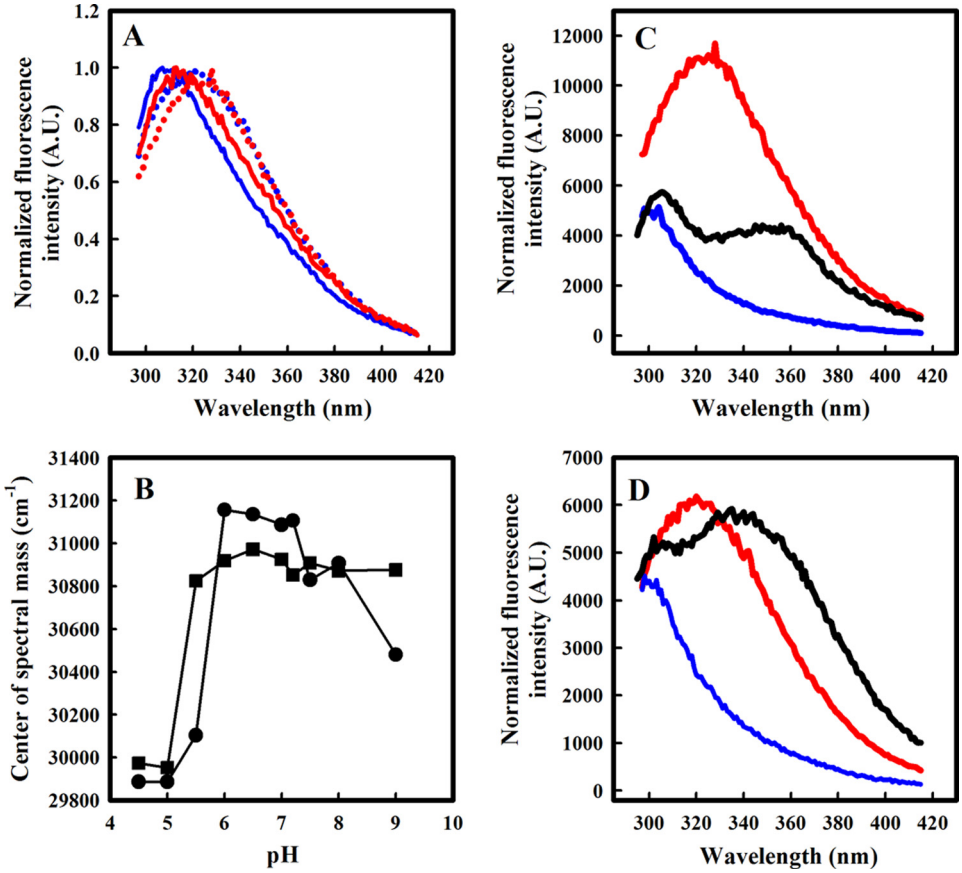

FIGURE 1. **pH-induced conformational changes of wt and R248Q p53C.** *A*, normalized intrinsic fluorescence emission spectra of wt p53C at pH 7.2 (*blue solid line*), wt p53C at pH 5.0 (*blue dotted line*), R248Q p53C at pH 7.2 (*red solid line*), and R248Q p53C at pH 5.0 (*red dotted line*). *B*, center of spectral mass values obtained from wt p53C (*circles*) and R248Q (*squares*) fluorescence emission spectra. Non-normalized intrinsic fluorescence emission spectrum of wt p53C (*C*) or R248Q p53C (*D*) is shown. Samples at pH 7.2 (*blue solid line*), at pH 5.0 (*red solid line*), and unfolded state (*black solid line*) (in *C*, with 6 M GdmCl; in *D*, 7 M urea) are shown. The samples were excited at 278 nm, and the emission was collected from 295 to 415 nm. All measurements were performed at 25 °C with 5 μM protein concentration.

exposed to the blot using the Enhanced Chemiluminescence (ECL) system (Roche Diagnostics).

Cell Transfection and Fluorescence Microscopy—The full-length p53-EGFP plasmid was obtained from the Genscript Corporation (Piscataway, NJ). Transient transfection experiments were performed with Fugene according to the manufacturer's recommendations (Roche Diagnostics). For analysis of GFP-p53, MCF-7 cells were plated onto glass-bottom dishes 48 h before the start of the experiment. Cells were then labeled with 75 nM LysoTracker (Invitrogen) and 10 μg/ml Hoechst (Molecular Probes) for 30 min. After labeling, cells were washed 3 times with phosphate-buffered saline. The images were then collected using an LSM 510 meta confocal microscope (Carl Zeiss International, Oberkochen, Germany). The LysoTracker red fluorescence excitation (ex) and emission (em) wavelengths were ~577 nm and ~590 nm, respectively. The Hoechst blue fluorescence wavelength was (ex/em 350/461 nm).

RESULTS

The Effect of pH on the Secondary and Tertiary Structures of wt and R248Q p53C—p53 is a very flexible protein that binds in a specific manner to more than 150 different genes (42). The core domain of p53 is known to be essential for sequence-specific DNA binding, and it contains several hot spot regions for mutation (43). For this reason, we investigated whether p53C can adopt alternative conformations and monitored p53C behavior using chemical perturbations. We previously investigated the behavior of the wt p53 core domain through the combination of high pressure and subzero temperature treatments, and we observed an alternative conformation that resembles the DNA-contact mutant R248Q p53C (9). R248Q is an excellent experimental model because this mutation is the most frequent one found in human cancers (6).

The tertiary conformations of wt and R248Q p53C were characterized by fluorescence spectroscopy at pH 5.0 and 7.2 (Fig. 1*A*). As expected, the fluorescence emission at pH 7.2 showed lambda maxima at 307 nm (wt) and 313 nm (R248Q), which indicates a native fold. This emission profile is characteristic of p53C because it represents eight tyrosine residues and one tryptophan in each core domain (2), and the tryptophan emission is highly quenched (Fig. 1*B*). At pH 5.0, the fluorescence spectra of wt and R248Q p53C display a significant red-shift (lambda maxima at 320 nm and 323 nm, respectively), indicating partial exposure of aromatic residues to the aqueous environment (44) (Fig. 1*A*). At low pH, there is also an increase in the fluorescence quantum yield (Fig. 1*C*). When the protein is denatured by high concentrations of urea or guanidine (Fig. 1, *C* and *D*, *black line*), the tryptophan is no longer quenched (has more intensity), the emission shifts to longer wavelengths (above 340 nm), indicating complete exposure to the solvent, and it is possible to distinguish the tyrosine emission from the tryptophan emission (two peaks). In contrast, the low pH conformation has a single peak at about 330 nm (average wavenumber = 30303 cm^{-1}), which is probably due to the location of the tryptophan in an average hydrophobic environment. The intensity of fluorescence increases at low pH, likely because the fluctuating structure of the molten-globule conformation prevents the quenching restrictions imposed by neighboring amino acid residues. On the other hand, the absence of a well-defined tyrosine peak at low pH (Fig. 1, *C* and *D*, *red line*) indicates that energy transfer occurs between the tyrosines and the tryptophan because the structure is still compact.

Fluorescence shifts can be quantified by determining the center of spectral mass (CM) of p53C fluorescence emission

spectra at different pH values. The CM values were maintained from pH 6.0 to 9.0 (Fig. 1*B*). In the pH range of 4.5 to 5.0, however, there is a sharp reduction of CM values (Fig. 1*B*). Similar results were observed for wt and R248Q p53C.

Additionally, we investigated pH-induced conformational changes by measuring binding to the hydrophobic probe, bis-ANS (Fig. 2). When bis-ANS is free in an aqueous medium, its fluorescence emission is negligible, but when it binds nonpolar residues in the proximity of positive charges, its fluorescence emission increases (45). This probe has been widely used to characterize intermediate states such as the MG conformation (21, 46, 47). Our data show that in the pH range from 4.5 to 5.0, binding of wt and mutant p53C to bis-ANS is 6-fold greater than at pH 6.0 to 9.0 (Fig. 2, *A* and *B*). In contrast, when the protein is denatured by urea, there is no binding of bis-ANS (Fig. 2*C*).

Because the MG conformation is characterized by maintenance of or increase in secondary structure (48, 49), we also measured circular dichroism to investigate structural changes due to low pH (Fig. 3). To follow changes in p53C predominantly β-sheet secondary structure, CD ellipticity values were monitored at 218 nm for p53C incubated at various pH values (Fig. 3, *A* and *B*). wt and R248Q p53C showed a significant increase in secondary structure at pH 5.0 (Fig. 3), an observation typical of other MG states (14, 19). There is a 1.7-fold gain in β-sheet secondary structure content for wt p53C at pH 5.0 in comparison with the same protein incubated at pH 7.2 as determined by the $[\theta]$ value obtained at 212 nm at both conditions.

This transition to a state with an increased negative ellipticity has been previously observed upon incubation with nondenaturing concentrations of guanidine hydrochloride (GdmCl) (29), and we observed the same transition with low concentrations of urea (supplemental Fig. S1).

p53C Presents a Higher Hydrodynamic Radius at Acidic pH—To investigate the hydrodynamic properties of p53C at pH 7.2 and pH 5.0, we analyzed the proteins by gel filtration chromatography (Fig. 4) and verified that both isoforms have a lower retention time at pH 5.0 than at pH 7.2 (Fig. 4 and data not shown), indicating that there is an increase in the hydrodynamic volume for both proteins at low pH. The data show a retention time of 13 min for the native conformation at pH 7.2 (Fig. 4, *solid line*), 12 min for the MG conformation (Fig. 4, *dotted line*), and 10 min for a completely denatured protein (Fig. 4, *dashed line*). The hydrodynamic radiuses (*Rg*) derived from the elution volumes and from the calibration of the column with standard proteins were: 1) 17.6 ± 0.5 Å for p53C at pH 7.2; 2) 19.3 ± 0.4 Å for p53C at pH 5.0; and 3) 30.9 ± 0.5 Å for denatured p53C.

The protein treated with 3 M guanidine has a greater hydrodynamic volume, as expected because of the less rigid structure than in the MG state. Taken together, these data clearly show that wt p53C and mutant R248Q can acquire an MG-like intermediate state in acidic pH.

Comparison of ^{1}H-^{15}N HSQC in Molten Globule and Native p53C States—The lack of fixed tertiary interactions in many globular proteins results in a fluctuating ensemble of structures (50). Although these molecules are heterogeneous, valuable structural information can be acquired through nuclear magnetic resonance (NMR) measurements. In general, folded proteins have good resonance signal dispersions and sharp peaks. MG states lose resonance signals and have much less signal dispersion. MG conformational heterogeneity is a result of residual secondary and side chain interactions; therefore, cross-peaks in the ^{15}N-^{1}H HSQC spectrum tend to be broad or dis-

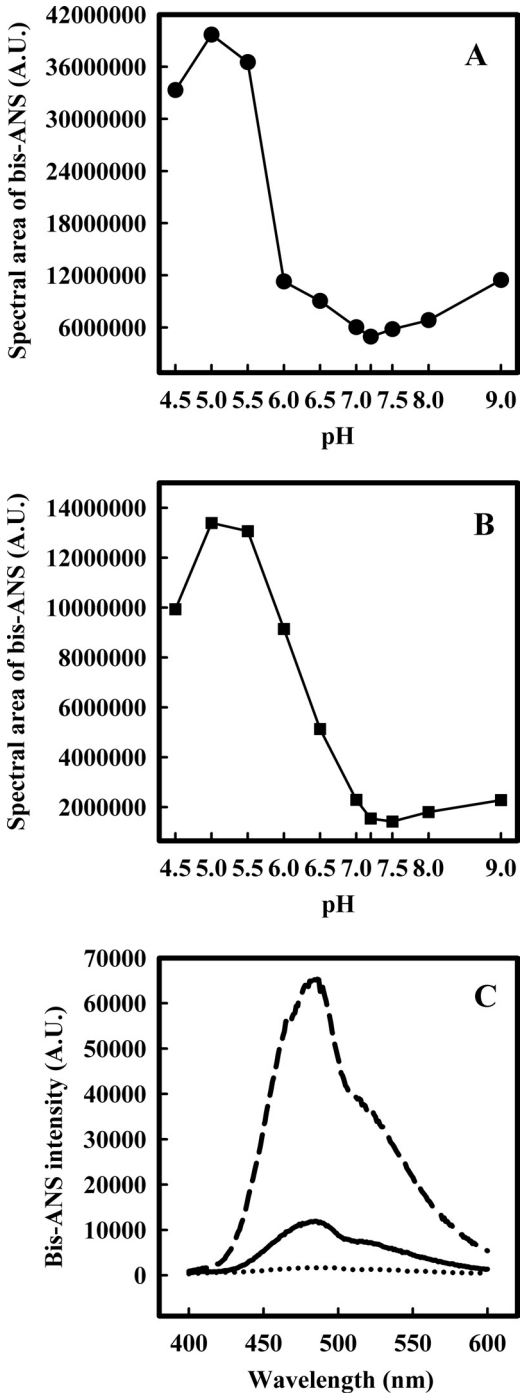

FIGURE 2. **Incubation at low pH exposes hydrophobic pockets.** *A*, total fluorescence intensity of bis-ANS bound to wt p53C (*circles*) or (*B*) R248Q p53C (*squares*). Proteins were incubated at 25 °C at several pH values. *C*, bis-ANS fluorescence emission spectrum in the presence of the hot-spot mutant, R248Q, at pH 5.0 (*dashed line*) and pH 7.2 (*solid line*). In contrast, when the protein was incubated with 6 M urea, there was no binding of bis-ANS (*dotted line*). The sample was excited at 360 nm, and the emission was measured from 400 to 600 nm. The R248Q and bis-ANS concentrations were both 5 μM.

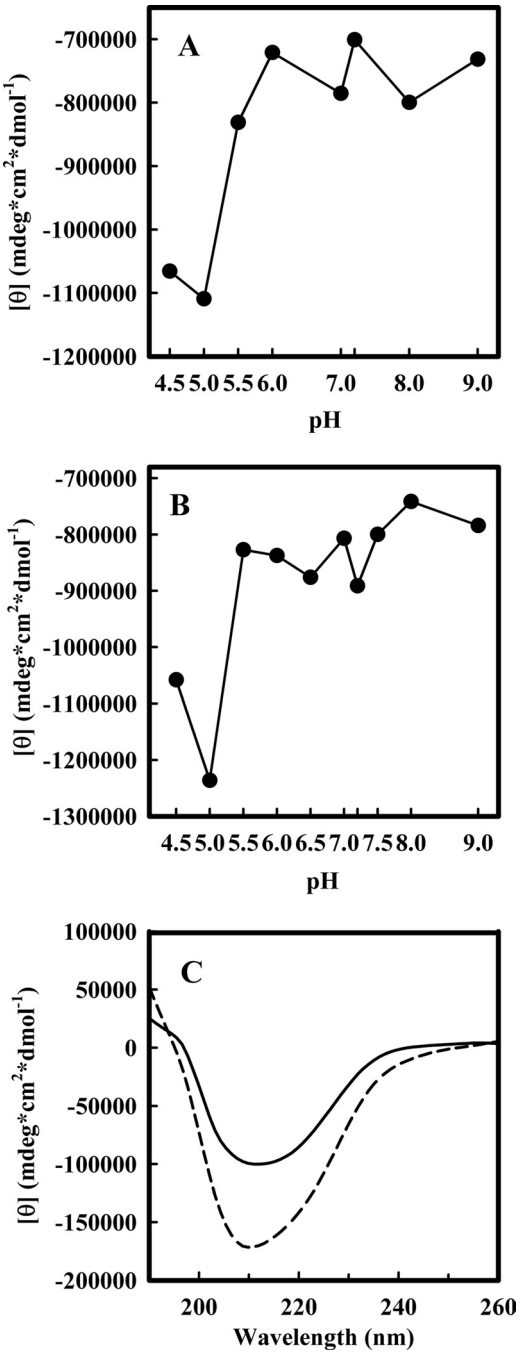

FIGURE 3. **Secondary structure of the MG state.** Wild-type (*A*) and R248Q p53C (*B*), at 10 μM, were incubated in solutions with different pH values, and the molar ellipticity at 218 nm was collected. *C*, circular dichroism spectra of wt p53C at pH 5.0 (*dotted line*) and pH 7.2 (*solid line*).

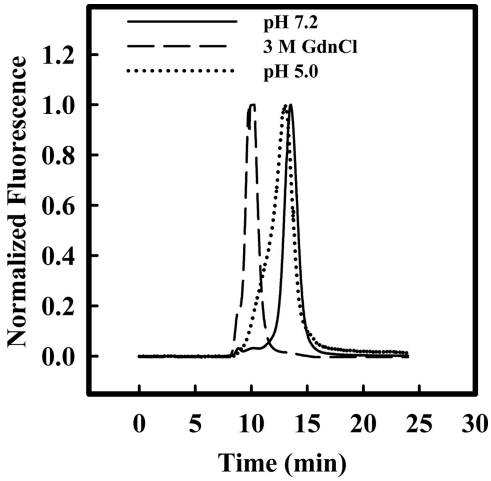

FIGURE 4. **Size-exclusion HPLC analysis of oligomeric states of native and MG p53C.** Normalized fluorescence at 280 nm was detected during gel filtration chromatography of wt p53C at pH 7.2 (*solid line*), pH 5.0 (*dotted line*), or incubated with 3 M GdmCl (*dashed line*).

appear completely (51). To further characterize the population of p53C molten globule structures at acidic pH, we carried out ^{15}N-edited NMR experiments of wt and R248Q p53C at pH 7.2 and 5.0 (Fig. 5). In the native state (blue), a broad distribution of resonance signals was observed, as previously described (52). At pH 5.0, there was a reduction in peak dispersion (Fig. 5, *red plot*). The wt p53C HSQC dispersion at pH 7.2 was observed from 10.142 to 6.075 ppm (^{1}H dimension), compared with 8.791 to 6.782 ppm (^{1}H dimension) at pH 5.0. We suggest that a broad set of peaks experiences different perturbations at pH 7.2 and represents the observed differences between pH 7.2 and 5.0, based on the backbone structure of wt p53C. Residues that have ^{1}H and ^{15}N chemical shifts at pH 5.0 are shown in violet (Fig. 5*B*). Curiously, the conformational changes are spread throughout the whole p53C structure (Fig. 5). In contrast, several residues of the MG state do not change significantly compared with the native state. The R248Q mutant, classified both as a contact and structural mutant (40), presented HSQC dispersion at pH 7.2 from 10.1360 to 6.6343 ppm and at pH 5.0 from 8.793 to 6.763 ppm (supplemental Fig. S2). These results were similar to those of the wild-type protein. Based on these data, we suggest that the MG states of both proteins (wt and R248Q p53C) are very similar. Subsequently, the samples were applied to a gel filtration column to analyze whether there were conformational transitions. Our data show that wt p53C at pH 7.2 has the same elution profile before and after HSQC measurement (data not shown). After the NMR experiment at pH 5.0, about 10–15% of the protein was in an oligomeric form. This result indicates that wt p53C can adopt different oligomeric states after longer incubation times at pH 5.0, probably because the MG is a flexible state, and some of the intramonomeric interactions are replaced by intermolecular interactions.

p53C Chemical and Physical Perturbations Allow Identification of Distinct Folded States—To analyze differences in the folding cooperativity and conformational stability of the molten globule and native p53C states, we studied the stability of the protein at different pH values against chemical (urea) and physical (pressure) treatments. Chemically induced unfolding of wt or R248Q p53C at pH 7.2 indicated that both proteins unfold to final CM values around 28,700 cm^{-1}. This value is compatible with the complete exposure of aromatic residues to the aqueous environment, suggesting that urea is able to induce complete unfolding. The unfolding of wt and R248Q p53C at pH 7.2 showed a cooperative, two-state denaturation process. The denaturation isotherms of wt and R248Q p53C at pH 5.0 occurred at lower urea concentrations and presented a lack of cooperativity (Fig. 6*A*) that is typical of a MG conformation.

It is also noteworthy that at pH 7.2, wt p53C is more resistant to pressure than the mutant (Fig. 6*B*). On the other hand, the

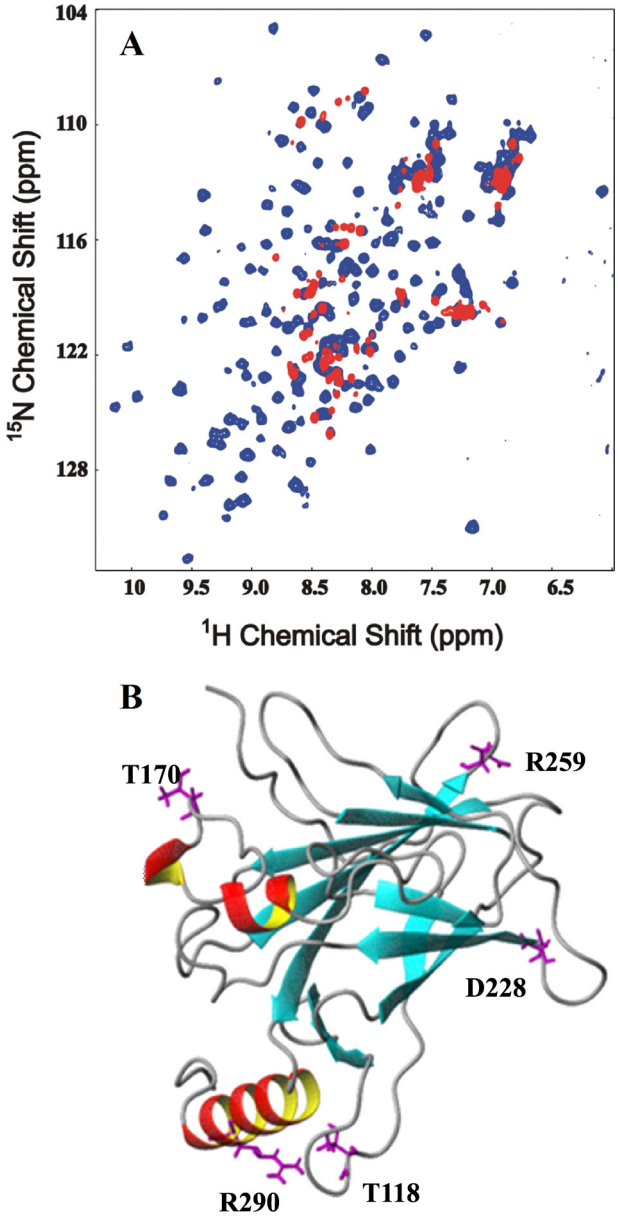

FIGURE 5. **Overlay of wt p53 ^{1}H-^{15}N HSQC spectra at different pH values.** *A*, *blue* and *red* spectra show wt p53C at pH 7.2 and 5.0, respectively. Compared with pH 7.2, pH 5.0 induced a reduction in the resonance signals and a decrease in the peak dispersions. *B*, representation of wt p53 core domain. ^{1}H-^{15}N HSQC correlation spectrum of p53C at pH 5.0 was compared with the p53C spectrum at pH 7.2. Residues that presented changes in amide chemical shifts at pH 5.0 are colored in *violet*.

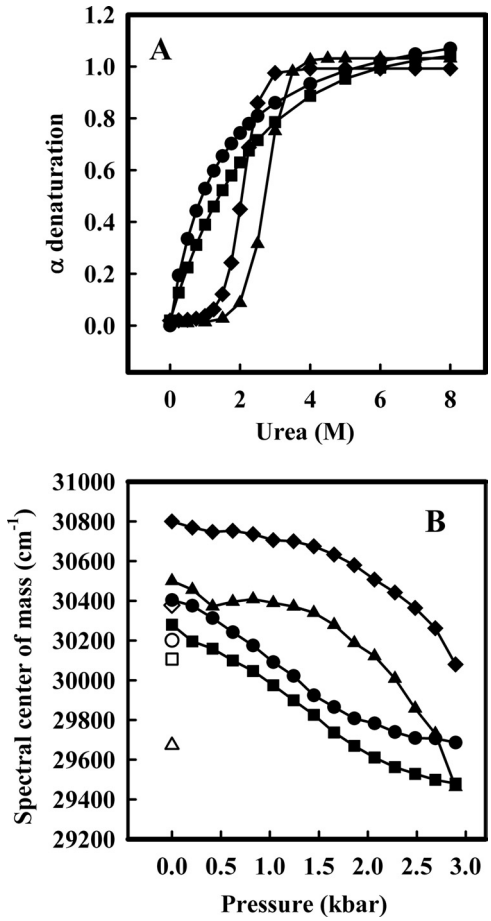

FIGURE 6. **Chemically and physically induced unfolding of wt and R248Q p53C.** Unfolding was monitored by intrinsic fluorescence and analyzed as the fraction (α) of denaturation for (*A*) chemical-induced unfolding or (*B*) CM values for pressure-induced unfolding. Wild-type p53C at pH 7.2 (*diamonds*) or pH 5.0 (*circles*) and R248Q at pH 7.2 (*triangles*) or pH 5.0 (*squares*) were incubated in: (*A*) the presence of different urea concentrations (0.5–8.0 M) or (*B*) compression up to 2.9 kbar. All measurements were performed at 25 °C with 5 μM protein. In *B*, open symbols correspond to CM values after the return to atmospheric pressure. To analyze the extent of denaturation (α), we used the following equation: $\alpha = \langle\nu\rangle - \langle\nu_i\rangle / \langle\nu_f\rangle - \langle\nu_i\rangle$, where $\langle\nu\rangle$ is the center of mass at each urea concentration, $\langle\nu_f\rangle$ is the center of mass in 8 M urea, and $\langle\nu_i\rangle$ is the center of mass in the absence of urea.

MG conformations of wt and R248Q (pH 5.0) were much less stable than the native conformations and had much smaller volume changes. Another interesting property is that at pH 5.0, the difference in stability is much smaller, and the reversibility is much higher (data not shown).

Localization of Full-length p53 in Acidic Cellular Compartments—To evaluate if p53 could be found in the acidic conformation in cells, we performed p53-GFP transfections into MCF-7 cells (human breast cancer). We used LysoTracker (Invitrogen) to probe acidic vesicles, as it is widely used to identify lysosomes with high specificity. After merging GFP fluorescence with the LysoTracker signal (Fig. 7), we observed that p53, which is expressed to high concentrations in the cell, tends to localize to acidic vesicles, mainly lysosomes (Fig. 7).

We also checked the cellular response to treatments with low pH (acid stress). We incubated MCF-7 cells at pH values 5.0, 6.0, and 7.2 for 24 h to identify their expression levels and p53 stabilization in the cell at different pH values. After total protein extraction, we performed Western blots with an anti-p53 antibody and observed a higher level of p53 at low pH (5.0), in comparison with the amount of p53 detected at pH 7.2 (Fig. 8). Because the level of p53-coding RNA did not change, it seems that low-pH stress leads to decreased proteolytic processing of the protein. Taken together, these two sets of data reveal the physiological importance for studying p53 at acidic pH.

DISCUSSION

The investigation of protein conformational changes has focused not only on understanding the unfolding and refolding

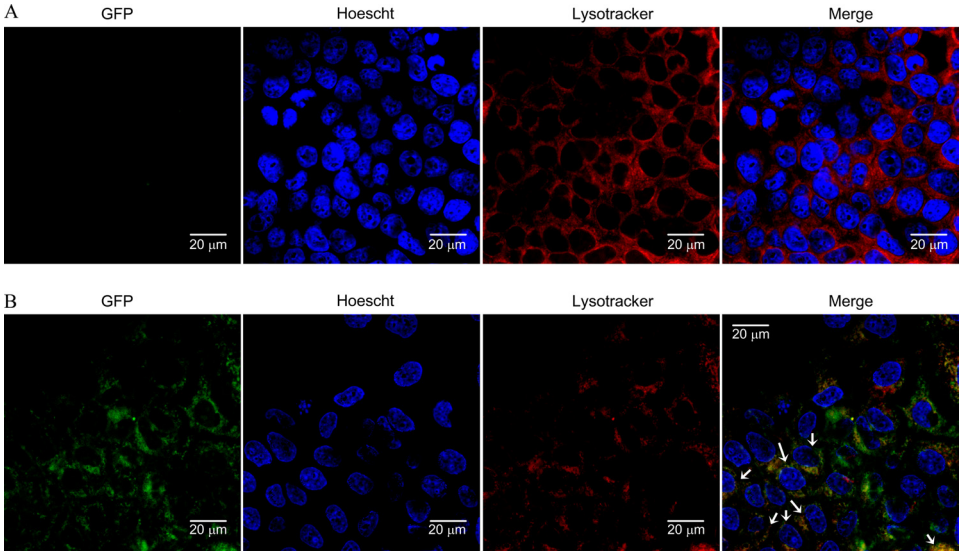

FIGURE 7. **Images of the p53-GFP-transfected cells with and without LysoTracker labeling.** Control, non-transfected MCF-7 (*A*) and GFP-p53-transfected MCF-7 (*B*) cells at pH 7.2 labeled with LysoTracker. In *A* and *B*, the images were obtained with an LSM 510 confocal fluorescence microscope. The *first panel* represents the *green channel* (GFP), the *second panel* represents the *blue channel* (Hoechst-labeled), the *third panel* represents the *red channel*, and the *fourth panel* shows the merging of GFP (*green channel*) and LysoTracker-labeling (*red channel*). *Arrows* indicate localization of p53-GFP in acidic vesicles.

of the main chain but also on identifying folding intermediates situated between the native and unfolded forms (26, 51, 53, 54).

Elucidation and characterization of intermediate states are important for understanding the mechanism of protein folding. These studies are crucial for proteins like p53 that have a large amount of flexibility associated with their function. Many folding intermediates are associated with neurodegenerative diseases such as Alzheimer, Parkinson, and prion-related encephalopathies, as well as some types of cancer (55–59). The mechanism of p53 folding has been previously studied (9, 11, 29, 60), but the exact folding pathway is not understood. We have isolated an intermediate state that is prone to aggregation through incubation with 1 M GdmCl (29), and we have also demonstrated that wt p53 can adopt a state similar to a mutant conformation when subjected to high hydrostatic pressure (HP) and subzero temperatures (9).

The p53 core domain is known to be very flexible; therefore, p53 can bind multiple protein targets such as BRCA1 (61), Hif-1 (62), Bcl-XL (63), 53BP1 or 53BP2 (64, 65), and Rad51 (66). These observations suggest that the core domain can acquire alternative conformations, and that the folding landscape might include partially folded, MG states. Based on this assumption, we used several techniques to present clear evidence of an MG conformation of the p53 core domain at acidic pH.

The MG state has been described as an intermediate conformation for a number of proteins. MGs are compact, denatured states with significant native-like secondary structure but with disrupted tertiary interactions (48, 49). Here, we show the molecular characteristics of the p53 MG state, inferred by loss of tertiary structure and native-like secondary structure content as well as bis-ANS binding (21, 48, 53). These results are relevant to the current literature in distinguishing the protein native and MG states. Through changes in protein radius, we describe the compact and partially folded state of p53C at acidic pH (Fig. 4). Analysis of the folded state suggests the critical importance of cooperativity. Urea isotherms clearly show that the protein presents a cooperative transition with two distinct states at pH 7.2, and that this transition becomes noncooperative when the chemical unfolding occurs at pH 5.0 (Fig. 6*A*). The difference in transition profiles indicates that there is an abrupt change in the p53C structure at pH 5.0, confirming the route to an intermediate state.

For some proteins, the partially folded and MG states play physiological roles. Structural modifications can be favorable, as in the case of the molten globule states of α-fetoprotein (AFP), α-lactoalbumin (67, 68), and folding chaperones (69, 70). The P22 phage Arc repressor protein is present physiologically in an equilibrium condition consisting of the native dimer and a monomeric MG species (21, 71, 72). In contrast, apoE4 forms a pathological MG conformation when it reaches the acidic pH of late endosomes, contributing to neurodegeneration in Alzheimer disease (73, 74). It has also been shown that the prion protein first adopts an MG state and then proceeds to a non-reversible β-sheet-rich form during oligomerization (75). These data highlight the importance of conformation in physiological and pathological processes.

In the case of the p53 core domain, the adoption of an MG conformation would be in line with its high flexibility and the potential to bind several ligands. The transition to a non-MG state at a pH above 5.5 would fix it in a conformation capable of acting as a transcription factor. In the case of the von-Hippel Lindau tumor suppressor protein (pVHL), Sutovsky and Gazit (18) demonstrated that the unbound conformation of the protein is an MG. Similar to p53, the lack of a fixed tertiary conformation allows pVHL to interact with a large number of proteins. It is important to note that not only the core domain but also the C-terminal domain of p53 is highly sensitive to changes in pH. The severity of the effect of the R337H mutation, which is responsible for the elevated incidence of adrenocortical carcinoma in South American children, depends on pH. These findings support a pH-dependent tumor suppressor function for this protein (76). If this conformation proves to have deleterious effects, a potential therapeutic strategy will be to use "structure correctors" to convert the pathological intermediate to a functional species. Because the wt and mutant molten-globule states exhibit similar stability and structural properties, this protein conformation may prove more useful as a target for compounds that will restore native function to the protein.

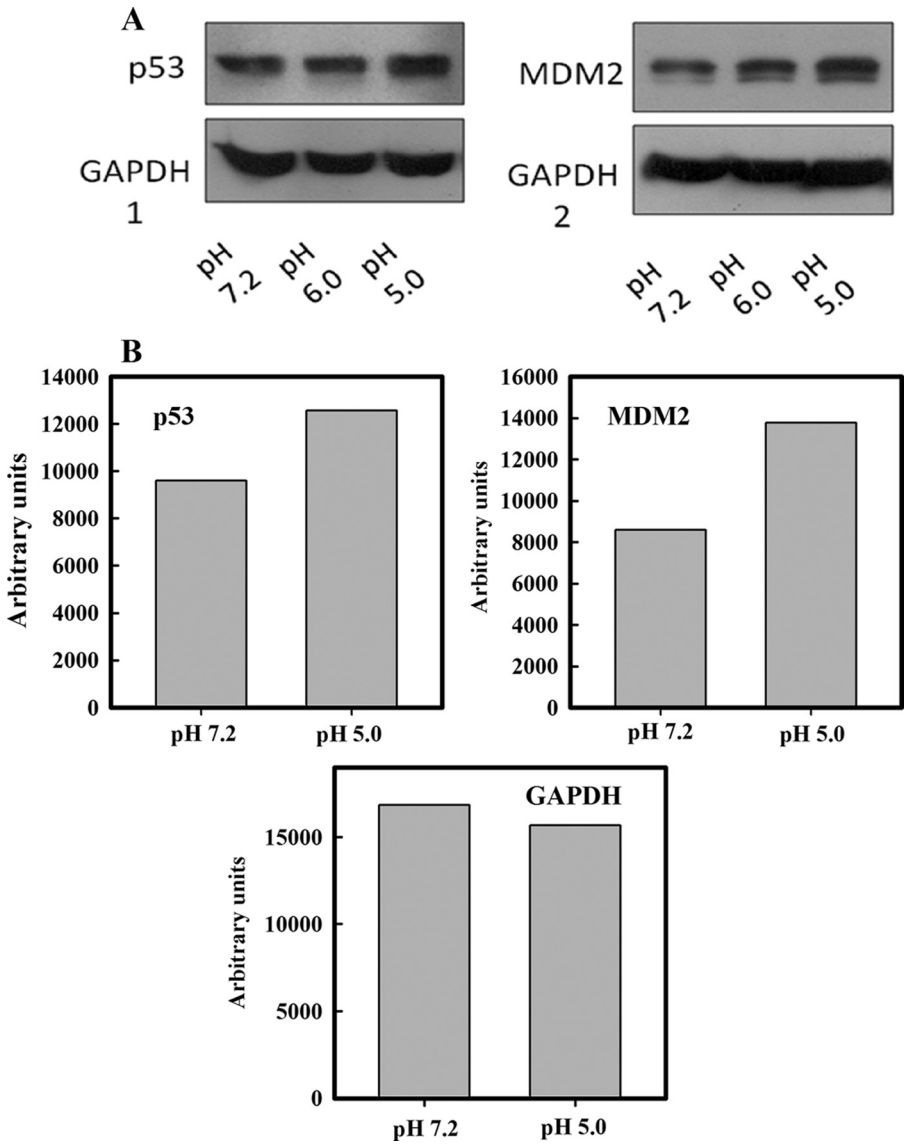

FIGURE 8. **Western blot analysis of full-length wt p53.** *A*, MCF-7 cells were incubated at pH 7.2, 6.0, or 5.0 for 24 h, and cellular extracts were evaluated for p53, MDM2, and GAPDH. *B*, quantification of the results shown in *A*, indicating that both p53 and MDM2 are present in higher amounts when cells are grown at pH 5.0 than at pH 7.2. These data are representative of three experiments.

but that pH variations promote conformational changes in this protein.

Most organelles, including the mitochondria, lysosomes, endoplasmic reticulum, and the Golgi apparatus, participate in the regulation of apoptosis. In 2002, Yuan *et al.* (83) demonstrated that p53-induced apoptosis occurred with lysosomal membrane permeabilization (LMP). LMP followed by the release of cathepsins into the cytosol is thought to be the key activation step of the lysosomal cell death pathway. These stimuli promote pH reduction and, consequently, caspase activation and mitochondrial membrane permeabilization, two classic apoptotic events (84). Therefore, the lysosomal cell death pathway has been suggested to represent a potential cancer target. p53 can be localized in the cytoplasm and nucleus. Accordingly, in the cytoplasm, p53 is found in mitochondria, in the proteasome, and, more recently, in the lysosome (84, 85). Our study reveals that p53 at pH 7.2 can be translocated into acidic vesicles (Fig. 7). Cells transfected with GFP-p53 were labeled with the fluorescent probe LysoTracker, which is used to visualize lysosomes. We found that GFP-p53 co-localizes with the lysosomal marker, suggesting p53 lysosome localization. In the acidic environment of the lysosome, the core domain of p53 will acquire a partially folded conformation. This acidic conformation is likely to be involved in the lysosomal cell death pathway.

p53 and Acidic pH Values in Tumoral Cells—There are several studies that correlate low pH values with cancer (77–79). Martinez-Zaguilan *et al.* (77) found that acidic environments induce metastasis in melanoma cells. Acidic pH values also lead to increases in interleukin-8 expression by human ovarian carcinoma cells (78) and induce expression of vascular endothelial growth factor (VEGF) in glioblastoma cells (79). There are reports that low pH increases the expression of p53 in tumoral cells (80–82). In human colonic adenoma-derived epithelial cells, there is an increase of p53 and p21 protein expression (80). Our findings showing that extracellular low pH stimulates increases in p53 (Fig. 8) are in line with these previous results.

Changes in pH have also been implicated in adrenocortical carcinoma (ACC) related to the R337H p53 mutation (76). It was proposed that R337H has a native conformation at pH 7.0,

Taken together, all of these data suggest that p53 may play physiological or pathological roles in acidic microenvironments. One possibility that can be considered is that the native wt p53 adopts a MG state when it interacts with the mitochondrial or lysosomal membrane during apoptosis or protein degradation. Another possibility is that native wt p53, in the presence of intratumoral acidic pH, is converted into an MG state, reducing or abolishing its function. We are currently utilizing single molecule approaches to further characterize the participation of the MG conformation of p53 in cellular function and disease.

Acknowledgments—We thank Dr. Fabio Almeida for help with NMR measurements and Emerson R. Gonçalves for competent technical assistance.

REFERENCES

1. Finlay, C. A., Hinds, P. W., and Levin, A. J. (1989) *Cell* **57,** 1083–1093
2. Cho, Y., Gorina S., Jeffrey, P. D., and Pavletich, N. P. (1994) *Science* **265,** 346–355
3. Laptenko, O., and Prives, C. (2006) *Cell Death Differ.* **13,** 951–961
4. Volgestein, B., Lane, D., and Levine, A. J. (2000) *Nature* **408,** 307–310
5. Levesque, A. A., and Eastman, A. (2007) *Carcinogenesis* **28,** 13–20
6. Soussi, T., Ishioka, C., Claustres, M., and Béroud, C. (2006) *Nat. Rev. Cancer* **6,** 83–90
7. Milner, J. (1995) *Trends Biochem. Sci.* **20,** 49–51
8. Klein, C., Georges, G., Künkele, K. P., Huber, R., Engh, R. A., and Hansen, S. (2001) *J. Biol. Chem.* **276,** 37390–37401
9. Ishimaru, D., Maia, L. F., Maiolino, L. M., Quesado, P. A., Lopez, P. C., Almeida, F. C., Valente, A. P., and Silva, J. L. (2003) *J. Mol. Biol.* **333,** 443–451
10. Ishimaru, D., Andrade, L. R., Teixeira, L. S., Quesado, P. A., Maiolino, L. M., Lopez, P. M., Cordeiro, Y., Costa, L. T., Heckl, W. M., Weissmüller, G., Foguel, D., and Silva, J. L. (2003) *Biochemistry* **42,** 9022–9027
11. Bullock, A. N., Henckel, J., and Fersht, A. R. (2000) *Oncogene* **19,** 1245–1256
12. Ishimaru, D., Ano Bom, A. P., Lima, L. M., Quesado, P. A., Oyama, M. F., de Moura Gallo, C. V., Cordeiro, Y., and Silva, J. L. (2009) *Biochemistry.* **48,** 6126–6135
13. Christensen, H., and Pain, R. H. (1991) *Eur. Biophys. J.* **19,** 221–229
14. Uversky, V. N. (2002) *Protein. Sci.* **11,** 739–756
15. Wright, P. E., and Dyson, H. J. (1999) *J. Mol. Biol.* **293,** 321–331
16. Engel, R., Westphal, A. H., Huberts, D. H., Nabuurs, S. M., Lindhoud, S., Visser, A. J., and van Mierlo, C. P. (2008) *J. Biol. Chem.* **283,** 27383–27394
17. Cremades, N., Bueno, M., Neira, J. L., Velázquez-Campoy, A., and Sancho, J. (2008) *J. Biol. Chem.* **283,** 2883–2895
18. Sutovsky, H., and Gazit, E. (2004) *J. Biol. Chem.* **279,** 17190–17196
19. Ptitsyn, O. B. (1995) *Adv. Protein Chem.* **47,** 83–229
20. Kuwajima, K. (1989) *Proteins.* **6,** 87–103
21. Silva, J. L., Silveira, C. F., Correia, A., Jr., and Pontes, L. (1992) *J. Mol. Biol.* **223,** 545–555
22. Dial, R., Sun, Z. J., and Freedman, S. J. (2003) *Biochemistry* **42,** 9937–9945
23. Fink, A. L. (1995) *Annu. Rev. Biophys. Biomol. Struct.* **24,** 495–522
24. Caramelo, J. J., Castro, O. A., Alonso, L. G., De Prat-Gay, G., and Parodi, A. J. (2003) *Proc. Natl. Acad. Sci. U.S.A.* **100,** 86–91
25. Silva, J. L., Oliveira, A. C., Gomes, A. M., Lima, L. M., Mohana-Borges, R., Pacheco, A. B., and Foguel, D. (2002) *Biochim. Biophys. Acta.* **1595,** 250–265
26. Ohgushi, M., and Wada, A. (1983) *FEBS Lett.* **164,** 21–24
27. Nam, G. H., and Choi, K. Y. (2002) *Eur. J. Biochem.* **269,** 5280–5287
28. Fink, A. L., Calciano, L. J., Goto, Y., Nishimura, M., and Swedberg, S. A. (1993) *Protein Sci.* **2,** 1155–1160
29. Ishimaru, D., Lima, L. M., Maia, L. F., Lopez, P. M., Ano Bom A. P., Valente, A. P., and Silva, J. L. (2004) *Biophys. J.* **87,** 2691–2700
30. Twigg, P. D., Parthasarathy, G., Guerrero, L., Logan, T. M., and Caspar, D. L. (2001) *Proc. Natl. Acad. Sci. U.S.A.* **98,** 11259–11264
31. Lo, M. C., Ha, S., Pelczer, I., Pal, S., and Walker, S. (1998) *Proc. Natl. Acad. Sci. U.S.A.* **95,** 8455–8460
32. Baleja, J. D., and Sykes, B. D. (1994) *Biochem. Cell Biol.* **72,** 95–108
33. Zhang, B., and Peng, Z. (1996) *J. Biol. Chem.* **271,** 28734–28737
34. Kim, P. S., and Baldwin, R. L. (1990) *Annu. Rev. Biochem.* **59,** 631–660
35. Nozaka, M., Kuwajima, K., Nitta, K., and Sugai, S. (1978) *Biochemistry* **17,** 3753–3758
36. Silva, J. L., Cordeiro, Y., and Foguel, D. (2006) *Biochim. Biophys. Acta.* **1764,** 443–451
37. Piotto, M., Saudek, V., and Sklenar, V. (1992) *J. Biomol. NMR*, **2,** 661–665
38. Delaglio, F., Grzesiek, S., Vuister, G. W., Zhu, G., Pfeifer, J., and Bax, A. (1995) *J. Biomol. NMR* **6,** 277–293
39. Johnson, B. A., and Blevins, R. A. (1994) *J. Biomol. NMR* **4,** 603–614
40. Wong, K. B., Dedecker, B. S., Freund, S. M., Proctor, M. R., Bycroft, M., and Fersht, A. R. (1999) *Proc. Natl. Acad. Sci.* **96,** 8438–8442
41. Pace, C. N. (1986) *Methods Enzymol.* **131,** 266–280
42. Meek, D. W. (2004) *DNA Repair* **3,** 1049–1056
43. Hollstein, M., Hergenhahn, M., Yang, Q., Bartsch, H., Wang, Z. Q., and Hainaut, P. (1999) *Mutat. Res.* **431,** 199–209
44. Lakowicz, J. R. (2006) *Principles of Fluorescence Spectroscopy*, pp. 529–575, Springer
45. Rosen, C. G., and Weber, G. (1969) *Biochemistry* **8,** 3915–3920
46. Da Poian, A. T., Oliveira, A. C., and Silva, J. L. (1995) *Biochemistry* **34,** 2672–2677
47. Hawe, A., Sutter, M., and Jiskoot, W. (2008) *Pharm Res.* **25,** 1487–1499
48. Creighton, T. E. (1997) *Trends Biochem. Sci.* **22,** 6–10
49. Arai, M., and Kuwajima, K. (2000) *Adv. Protein Chem.* **53,** 209–282
50. Kim, S., Bracken, C., and Baum, J. (1999) *J. Mol. Biol.* **294,** 551–560
51. Kamatari, Y. O., Kitahara R., Yamada, H., Yokoyama, S., and Akasaka, K. (2004) *Methods* **34,** 133–143
52. Rippin, T. M., Freund, S. M., Veprintsev, D. B., and Fersht A. R. (2002) *J. Mol. Biol.* **319,** 351–358
53. Vassilenko, K. S., and Uversky, V. N. (2002) *Biochim. Biophys. Acta.* **1594,** 168–177
54. Herczenik, E., and Gebbink, M. F. (2008) *FASEB J.* **22,** 2115–2133
55. Dobson, C. M. (1999) *Trends Biochem. Sci.* **24,** 329–332
56. Foguel, D., Suarez, M. C., Ferrão-Gonzales, A. D., Porto, T. C., Palmieri, L., Einsiedler, C. M., Andrade, L. R., Lashuel, H. A., Lansbury, P. T., Kelly, J. W., and Silva, J. L. (2003) *Proc. Natl. Acad. Sci. U.S.A.* **100,** 9831–9836
57. Cordeiro, Y., Kraineva, J., Ravindra, R., Lima, L. M., Gomes, M. P., Foguel, D., Winter, R., and Silva, J. L. (2004) *J. Biol. Chem.* **279,** 32354–32359
58. Foguel, D., and Silva, J. L. (2004) *Biochemistry.* **43,** 11361–11370
59. Chung, C. M., Chiu, J. D., Connors, L. H., Gursky, O., Lim, A., Dykstra, A. B., Liepnieks, J., Benson, M. D., Costello, C. E., Skinner, M., and Walsh, M. T. (2005) *Biophys J.* **88,** 4232–4242
60. Bullock, A. N., Henckel, J., DeDecker, B. S., Johnson, C. M., Nikolova, P. V., Proctor, M. R., Lane, D. P., and Fersht, A. R. (1997) *Proc. Natl. Acad. Sci. U.S.A.* **94,** 14338–14342
61. Chai, Y. L., Cui, J., Shao, N., Shyam, E., Reddy, P., and Rao, V. N. (1999) *Oncogene* **18,** 263–268
62. Hansson, L. O., Friedler, A., Freund, S., Rudiger, S., and Fersht, A. R. (2002) *Proc. Natl. Acad. Sci. U.S.A.* **99,** 10305–10309
63. Petros, A. M., Gunasekera, A., Xu, N., Olejniczak, E. T., and Fesik, S. W. (2004) *FEBS Lett.* **559,** 171–174
64. Iwabuchi, K., Li, B., Massa, H. F., Trask, B. J., Date, T., and Fields, S. (1998) *J. Biol. Chem.* **273,** 26061–26068
65. Glover, J. N., Williams, R. S., and Lee, M. S. (2004) *Trends Biochem. Sci.* **29,** 579–585
66. Buchhop, S., Gibson, M. K., Wang, X. W., Wagner, P., Stürzbecher, H. W., and Harris, C. C. (1997) *Nucleic Acids Res.* **25,** 3868–3874
67. Gillespie, J. R., and Uversky, V. N. (2000) *Biochim. Biophys. Acta.* **1480,** 41–56
68. Svensson, M., Sabharwal, H., Håkansson, A., Mossberg, A., Lipniunasi, P., Leffler, H., Svanborg, C., and Linse, S. (1999) *J. Biol. Chem.* **274,** 6388–6396
69. Bochkareva, E. S., Lissin, N. M., and Girshovich, A. S. (1988) *Nature* **336,** 254–257
70. Rawat, U., and Rao, M. (1998) *J. Biol. Chem.* **273,** 9415–9423
71. Burgering, M. J., Hald, M., Boelens, R., Breg, J. N., and Kaptein, R. (1995) *Biopolymers.* **35,** 217–226
72. Milla, M. E., and Sauer, R. T. (1995) *Biochemistry* **34,** 3344–3351
73. Ditaranto, K., Tekirian, T. L., and Yang A. J. (2001) *Neurobiology of Disease* **8,** 19–31
74. Ji, Z. S., Müllendorff, K., Cheng, I. H., Miranda, R. D., Huang, Y., and Mahley, R.W. (2006) *J. Biol. Chem.* **281,** 2683–2692
75. Gerber, R., Tahiri-Alaoui, A., Hore, P. J., and James, W. (2007) *J. Biol. Chem.* **282,** 6300–6307
76. DiGiammarino, E. L., Lee, A. S., Cadwell, C., Zhang, W., Bothner, B., Ribeiro, R. C., Zambetti, G., and Kriwacki, R. W. (2002) *Nat. Struct. Biol.* **9,** 12–16
77. Martínez-Zaguilán, R., Seftor, E. A., Seftor, R. E., Chu, Y. W., Gillies, R. J.,

and Hendrix, M. J. (1996) *Clin. Exp. Metastasis* **14,** 176–186
78. Xu, L., and Fidler, I. J. (2000) *Cancer Res.* **60,** 4610–4616
79. Xu, L., Fukumura, D., and Jain, R. K. (2002) *J. Biol. Chem.* **277,** 11368–11374
80. Williams, A. C., Collard, T. J., and Paraskeva, C. (1999) *Oncogene* **18,** 3199–3204
81. Ohtsuho, T., Wang, X., Takahashi, A., Ohnishi, K., Saito, H., Song, C. W., and Ohnishi, T. (1997) *Cancer Res.* **57,** 3910–3913
82. Choi, E. K., Roberts, K. P., Griffin, R. J., Han, T., Park, H. J., Song, C. W., and Park, H. J. (2004) *Int. J. Radiat. Oncol. Biol. Phys.* **60,** 1264–1271
83. Yuan, X. M., Li, W., Dalen, H., Lotem, J., Kama, R., Sachs, L., and Brunk, U. T. (2002) *Proc. Natl. Acad. Sci. U.S.A.* **99,** 6286–6291
84. Kroemer, G., and Jäättelä, M. (2005) *Nat. Rev. Cancer* **5,** 886–897
85. Mihara, M., and Moll, U. M. (2003) *Methods Mol. Biol.* **234,** 203–209